INITIAL PHASE ANALYSIS OF R WAVES FROM GREAT EARTHQUAKES

Abbreviated title: Initial Phase Analysis of R waves

Muneyoshi FURUMOTO

Department of Earth Sciences
Faculty of Science
Nagoya University,
Chikusa, Nagoya 464,
Japan

ABSTRACT

The phase equalization was carried out for R waves in order to obtain the information on the source mechanisms of the four earthquakes, the Kurile earthquake of 1963, its largest aftershock, the Rat Is. earthquake of 1965, and the Tokachi-oki earthquake of 1968. Initial phase was computed using the corresponding complete great-circle phase velocity, so that the influences of the lateral heterogeneity of the earth's structure were considerably reduced. The fault length of the Kurile earthquake was determined from the initial phase radiation pattern on the basis of a simple propagating fault model. There is no trade= off in this method between the fault length and the rupture velocity. Such a trade-off is inherent to the conventional directivity method. A fault length of 250 Km was obtained, which was found to be nearly equal to the length of the aftershock area. We have introduced a dynamic fault parameter 'source time' that can be determined from the phase measurement using the complete great-circle phase velocity rather than the average phase velocity of the individual multiple R waves. This quantity corresponds to the rise time of the source time function of an equivalent point source. Source times of 97, 62, 174, and 115 sec were obtained for the above four earthquakes.

INTRODUCTION

A major problem in seismology is the credible extraction of source information from various seismic signals. For this purpose, diverse analyses of long-period surface waves (G and R waves) have been experimented. One of the methods is to determine the initial phase angles of the waves, invoking the method of the phase equalization (Brune,1960; Aki,1962; Ben-Menahem et al.,1968). However, seismologists seem to attach less importance to the phase analyses. The chief reason may be the uncertainty in the phase velocity data on the signal paths which makes the measurement and the interpretation of the obtained initial phases difficult (Aki,1962). Primarily because of the lateral heterogeneity of the earth's structure, use of the dispersion curve constructed for a laterally homogeneous model of the earth does not warrant an accurate equalization of phases. This problem is especially serious for a study of very large earthquakes. The available records of G and R waves are usually multiple signals travelling very long distances along the great-circles so that the equalization process by a model dispersion may accumulate a significant error in determining the initial phase.

Although the phase analysis contains such a difficulty, it should provide important information on the source mechanism. The initial phase is a sensitive function of the spatial and the temporal expansion of the fault. Some of the related source parameters can be determined, in principle, more definitely by the phase analysis than the conventional amplitude analyses. In this paper, we will show that a fault length and a source time duration can be estimated very reliably from the phase data of R waves. We employed, in order to minimize the influences of the lateral heterogeneity, the R wave records for which the phase velocity data on the complete great-circle paths are available. The earthquakes studied are the Kurile earthquake of 1963, its largest aftershock, the Rat Island earthquake of 1965, and the Tokachi-oki earthquake of 1968. These earthquakes excited R waves large enough to be used for an accurate analysis. Table 1 shows the data pertinent to the four sources.

DATA AND PHASE EQUALIZATION

Nakanishi (1978a,b,1979) analyzed many R wave records of the four events in order to determine the complete great-circle phase velocity and the quality factor Q. We employed the same set of the digitized data so that his results for the phase velocity (Nakanishi,1978a, 1979) can be directly referred. We therefore describe only the outline of the data processing whose detail is given in Nakanishi (1978a,1979). The multiple R wave signals were separated from the long-period vertical seismograms of World Wide Standard Seismographic Network (WWSSN) through the group velocity window of the range 3.45 - 3.90 Km/sec. The signals were digitized and an equal interval interpolation was performed at $\Delta t=4$ sec. Stations used are listed in Tables 2 to 5 with other related information. Using a new technique of time series analysis, Nakanishi (1978a,b,1979) computed the complete great-circle phase velocity from such a pair of the signals as R_n and R_{n+2} .

The numerical procedure for the phase equalization method has been described by Ben-Menahem et al.(1968). We recapitulate the salient points of the method. The digitized traces were smoothed over three points and then the phase spectra $\Psi(\omega)$ were computed by the

fast Fourier transform method. The initial phase $\Phi(\omega)$ can be obtained from the phase angle $\Psi(\omega)$ by

$$\Phi(\omega) = \Psi(\omega) - \omega t_1 + \frac{\omega r}{c(\omega)} + \phi_s(\omega) - \frac{m}{2}\pi \pm 2N\pi \qquad (1)$$

where ω; the angular frequency

t_1; the initial time of the group velocity window

c; the phase velocity

r; the travel distance of the wave

ϕ_s; the instrumental phase delay

$\frac{m}{2}\pi$; the polar phase shift.

The distance r was computed from the epicentral distance and the length of the complete great-circle (Tables 2-5). Before the calculation of the transmission factor $\omega r/c$, the observed phase velocities (Nakanishi,1978a,b,1979) were smoothed and interpolated as follow. We calculated firstly the velocity difference Δc between the observation and the theoretical dispersion for the structural model 5.08M (Kanamori,1970a), which is fully smooth. Secondly the difference was approximated by the second order series of frequency $\Delta c = a_2 f^2 + a_1 f^1 + a_0$ in a range of 0.0033 - 0.0059 Hz. The final phase velocity was obtained by adding this Δc to the theoretical phase velocity ($c(\omega) = c_{5.08M} + \Delta c$). Since the travel path consists of the complete great-circle and the excess

part, either the major or the minor arc, the phase velocity obtained above is not always the best value for the phase equalization. The best one may be the average phase velocity weightened with the path lengths on the basis of a regionally heterogeneous earth model (Kanamori,1970a; Nakanishi,1979). The error from the usage of the great-circle phase velocity, however, would be small, because the excess travel path is relatively short as compared to the whole travel path. This error can be estimated as follow. Let δc be the difference between the average phase velocity of the excess path and the used great-circle phase velocity. The use of the latter phase velocity gives an error of $\delta\Phi$ in the initial phase determination:

$$\delta\Phi = \delta\left(\frac{\omega r}{c}\right) = -\omega r \frac{\delta c}{c^2} \qquad (2)$$

where the distance r is the length of the excess travel path. If we take r=10000 Km, c=4.9 Km/sec, and δc=0.01 - 0.02 Km/sec at T=250 sec, the expected error would be $\delta\Phi$ = 0.1 - 0.2 (radian).

The instrumental phase delay was computed from the equation by Hagiwara (1958). As indicated under Tables 2 to 5, the two types of the seismographs were operated under WWSSN in the period 1963 - 1968; one had

a period of the free oscillation of the pendulum T_p= 30 sec, and the other T_p= 15 sec. Other constants characterizing the instrumental responses were cited from Chandra (1970). We checked the theoretical responses thus obtained against the actual calibration curves on all the seismograms of the largest after-shock of the Kurile event of 1963 and of the Tokachi-oki earthquake of 1968. We found that the long-period seismographs of WWSSN were in general set in remarkably good conditions. Although the differences are minor, we used the instrumental phase delays determined from the actual calibration curves for the above two events.

RADIATION PATTERN OF INITIAL PHASE

Ben-Menahem and his colleagues discussed the radiation pattern of the initial phase in their serial works (Ben-Menahem,1961; Ben-Menahem and Harkrider,1964; Ben-Menahem *et al.*,1970). The radiation pattern is essentially composed of two factors. The first factor depends upon the focal mechanism and, with a minor significance, the focal depth. It may be noted that Ben-Menahem and his colleagues called only this term the 'initial phase'. The other is the finiteness factor, which arises from the finiteness of the source.

This second factor can be expressed as follow for such a simple source model that the rupture moves horizontally with a uniform velocity over a finite fault length (Ben-Menahem,1961).

$$\phi_f(\omega,\theta) = -\frac{\omega L}{2v_r} + \frac{\omega L}{2c}\cos\theta \qquad (3)$$

where L is the fault length, v_r the rupture velocity, c the phase velocity at an angular frequency ω, and θ the angle between the great-circle and the rupture direction (the fault strike). The cosine type asymmetry of the initial phase radiation pattern is diagnostic of the fault length. One can use equation (3) to get the rupture length without any trade-off with the rupture velocity. In practice it is necessary for using (3) to perform an accurate phase equalization (Aki,1962). The focal mechanism must be known beforehand. The former requirement was achieved using the complete great-circle phase velocity data. The focal mechanism has been determined from the body wave data and the amplitude data of long-period surface waves (e.g. Kanamori,1970b).

The initial phases of the Kurile earthquake are plotted in radian against the azimuth in Fig.1. The data points indicate the averages at period around

T = 250 sec (T = 273,256,241, and 228 sec), where one can expect the most precise determination of the phase velocity. Fig.1 clearly shows the performance of the accurate phase equalization since the points distribute in a remarkably narrow range along the general trend of the azimuthal pattern. The points between azimuths 45 - 65° deviate from the general trend. The corresponding great-circles cover tectonically very active regions such as the Kurile arc, the Aleutian arc, and the western coasts of the North and South American Continents. A strong regional variation of phase velocity can be expected for these paths, where the complete great-circle phase velocity may not be adequate approximation for the average phase velocity of the individual multiple R waves. A strong lateral refraction of the waves can also be expected for these paths and may be partly responsible for the above deviation. We excluded the related data from the analysis.

The focal mechanism factor of the initial phase can be calculated from the numerical tables of Ben-Menahem et al. (1970) with the focal mechanism solution (dip-direction ϕ=317°, dip-angle δ=22-45° pure dip= slip motion; Abe et al,1970; Kanamori,1970b; Stauder and Mualchin,1976). The result shows that the mechanism factor has a small asymmetry of the radiation pattern,

the amplitude of the asymmetry being about 0.1 (radian). Therefore the observed large asymmetry should be largely explained by the finiteness factor. We fitted a cosine function curve to the data points by the least squares method. The constant term of the radiation pattern was fixed at a value obtained by the technique described in the next section. For the best fitted curve, the amplitude and the direction of the maximum phase are 0.65 (radian) and 65° respectively (Fig.1). Then the fault length is computed immediately to be L=250 Km (ω = 0.0251 sec^{-1} and c = 4.9 Km/sec). As indicated by equation (3), the azimuth of the maximum phase (θ = 0°) corresponds to the rupture direction. The fault length of 250 Km and the rupture direction of 65° are consistent with the results of Kanamori (1970b) and Ben-Menahem and Rosenman (1972) who used the amplitude radiation pattern or the directivity function of long-period surface waves. The feature also agrees well with the shape of the aftershock area (Fig.2). It should be noted that in Kanamori (1970b) and Ben-Menahem and Rosenman (1972) the fault length was not uniquely determined but largely constrained by the aftershock area. Generally, the approximate equality between the length of the fault and the aftershock area has been demonstrated by the geodetic data (Plafker,1972;

Shimazaki,1974) or the tsunami source data (Hatori,1970; Abe,1973) rather than the seismic wave data. Such an equality, however, was demonstrated in the present case soly from the initial phase radiation pattern of long= period seismic waves.

The initial phases of the largest aftershock of the Kurile earthquake are plotted in Fig.3. The curve fitting is somewhat difficult in this case. Since the aftershock excited much smaller R waves than the main shock, the determination of the initial phases would be subjected to larger errors. Furthermore, a small finiteness factor due to a small fault gives only a small asymmetry of the radiation pattern. Hence the finiteness factor was calculated on the assumption that the fault ruptured southwards over a length of 100 Km. Such a fault model is appropriate in view of the aftershock distribution following this aftershock (Fig.2; Fukao,1979). The result is illustrated by the solid curve in Fig.3. Although the curve contains only the finiteness factor, it alone accounts for the observed initial phases. This fact implies that the mechanism factor is nearly constant with respect to the azimuth. Such an approximate constancy is realized when both nodal planes of the focal mechanism have moderate dip-angles. Mechanism factor for a impulsive source is represented as follow (equation

(50) of Ben-Menahem et al.,1970).

$$\phi_m = -\frac{\pi}{4} + \tan^{-1}\left[\frac{qQ_R}{sS_R + pP_R}\right] \qquad (4)$$

where q,p, and s are given from the mechanism solution, and Q_R,P_R, and S_R by the numerical tables (Ben-Menahem et al.,1970). If the source is a pure dip-slip fault with a dip-angle of $\delta=45°$, then $qQ_R=0$ and $sS_R+ pP_R< 0$ for all azimuths. Then the phase ϕ_m for a source of a step function type becomes constant, as

$$\phi_m = -\frac{3\pi}{4} - \pi = -\frac{7}{4}\pi \qquad (5)$$

On the contrary, a very steeply dipping nodal plane ($\delta=87°$) was almost unambiguously determined from the first motion data (Stauder and Mualchin,1976). Although the other nodal plane was not determined accurately, any large amount of strike-slip component is inconsistent with the data. A simple and reasonable mechanism consistent with the first motion data is therefore a thrust fault with a dip-angle as low as 3° (Fukao,1979). The dotted curve in Fig.3 indicates the focal mechanism factor in this case. It is clear that the observation by no means supports such a mechanism. The disagreement can be explained by a focal mechanism

change through the rupture process from very low-angle thrusting to moderate- or high-angle thrusting. The directions of the first motions give the mechanism at the beginning of the rupture, while the radiation pattern of long-period surface waves reflects the mechanism averaged over the entire process. The mechanism change has been also supported by the amplitude radiation pattern of long-period Love waves and long-period P waveforms (Fukao,1979). Fukao (1979) discussed on the significance of the development of moderate angle thrusts near deep sea trenches from the tectonical point of view.

For the other two earthquakes, the radiation pattern analysis was not carried out, because the azimuthal coverage of high quality R waves data is poor. Especially for the Rat Is. earthquake the data at azimuths near the rupture direction are sparse due to a too large asymmetry of the amplitude radiation pattern (Wu and Kanamori,1973).

SOURCE TIME

Consider a couple of R waves of vertical component radiated in opposite directions from a source, like R_2 and R_3 waves. For an instantaneous point source, the sum of their initial phases is $\pi/2$ regardless of the focal mechanism (Ben-Menahem et al.,1968). We mean by an instanteneous point source a double couple force

acting at a point stepwise in time. If the source has a finite source process time τ, the sum becomes $(\pi/2 - \omega \cdot \tau)$, where ω is angular frequency. Therefore the difference between the observed sum and $\pi/2$ gives the source time τ. The sum of the initial phases can be computed accurately using such a pair of R waves as R_n and R_{n+1}. For example, take R_2 and R_3 waves at a given station. Their travel distances are d_2 and d_1+D, where d_2 is the length of the major arc of the great-circle, d_1 the length of the minor arc, and D the length of the complete great-circle ($D=d_1+d_2$). The transmission factors are $\omega d_2/c_2$ and $\omega(d_1/c_1+D/c)$, where c_1, c_2, and c are the average phase velocities on the paths corresponding to d_1, d_2, and D, respectively. In order to calculate the sum of the initial phases, we need to know the sum of the transmission factors, $\omega d_2/c_2 + \omega(d_1/c_1+D/c)$. This sum can be calculated without any individual knowledge of c_1 and c_2, since

$$\omega d_2/c_2 + \omega(d_1/c_1 + D/c) = \omega(d_2/c_2 + d_1/c_1) + \omega D/c$$
$$= \omega D/c + \omega D/c \qquad (6)$$

Because we know the precise phase velocity c, there exists no uncertainty in the calculation of the above sum. This convenience comes from the fact that the sum of the

travel distances of R_n and R_{n+1} waves consists of the just n-times the complete great-circles. Furthermore, the errors in the epicentre location do not affect the sum of the initial phases of R_n and R_{n+1} waves, because their effects are canceled by each other. However, the error of the origin time of an earthquake directly affects the estimation of the sum, though it may be generally small. We postulate that the source time τ defined here is a very useful quantity for measuring the duration of a great earthquake.

In order to see in more detail the physical meaning of the source time τ, we consider a simple finite source model. The model is a rectangular fault with the length L, the width W, the rupture velocity v_r, and the rise time τ_R of a linear ramp function (Haskell,1964). Rupture is assumed to occur instantaneously in the width direction and to propagate horizontally along the length. The source time τ is separated into three terms characterizing the finite source process. The simple source process (Haskell model) is characterized by two duration times τ_L and τ_R associated with the fault length and the rise time respectively. The other important term comes from a delay of the main rupture propagation. For the Tokachi-oki earthquake of 1968, Fukao and Furumoto (1975) observed a substantial time lag

between the onset of the shock and the initiation of the main rupture propagation. Because it is this main rupture that contributes to the generation of long-period surface waves (Fukao and Furumoto,1975), the delay time τ_D of the main rupture propagation is a significant factor of the source time. The source time τ thus consists of the three terms.

$$\tau = \tau_L + \tau_R + 2 \cdot \tau_D \qquad (7)$$

It should be noted that, even if $\tau_D \neq 0$, the source time τ defined by equation (7) can be regarded in a broad sense as a rise time of the equivalent point source (Fig.4). The source attains a half of the eventual seismic moment ($M_o/2$) after a time of $\tau/2$, though the ultimate seismic moment M_o is achieved after a time of $\tau_L+\tau_R+\tau_D$.

The duration time τ_L can be interpreted as a time required for the main rupture to propagate along the fault length. Since the four events are all unilateral faults (Kanamori,1970b,1971; Wu and Kanamori,1973), the rupture time τ_L is represented by the ratio of the fault length to the rupture velocity, L/v_r. The rupture times τ_L of the three great earthquakes, the Kurile earthquake, the Rat Is. earthquake, and the Tokachi-oki earthquake, have been determined to be about 70 sec,

120-140 sec, and 40 sec, respectively (Kanamori,1970b, 1971; Ben-Menahem and Rosenman,1972; Wu and Kanamori,1973). We employed the relation $\tau_R = W/2v_r$, which has been suggested by Savage (1972), in order to determine the rise time of a great earthquake. Fukao and Furumoto (1979) determined the rise time of the great Etorofu (Iturup) earthquake of November 6, 1958, using relatively short-period surface waves at short distances. They obtained a value of τ_R which is approximately equal to $W/2v_r$. The fault width W is assumed to be equal to the width of the aftershock area (Table 6) and a rupture velocity v_r= 3.5 Km/sec is adopted. The calculated rise time τ_R is about 20 sec, 20 sec, and 10 sec for the Kurile earthquake, the Rat Is. earthquake, and the Tokachi-oki earthquake, respectively.

In the present study the source time τ was computed at seven points in the period range 273 - 195 sec. The computed values of τ for the Kurile earthquake are plotted for the three stations, AAE, ADE, and KON, in Fig.5. They give the second longest (AAE), an average(KON), and the shortest (ADE) estimation of the source time τ. As shown in the figure, the computed values are satisfactorily uniform with respect to the period for each station. The average of τ for each station is plotted as a function of azimuth in Figs. 6 to 9 for the four earthquakes. The solid line in each

figure represents the ultimate average of the source time τ (Table 6), which gives the constant term of the initial phase radiation pattern (Figs.1 and 3). In the case of the Kurile earthquake of 1963 we obtained τ=97 sec. In Fig.1, however, the constant term was calculated from the value of τ = 93 sec, an average obtained by excluding the results from the three stations (GOL, LPS, and TUC), which lie in the azimuthal range of 45 - 65°. As shown in Figs. 6 to 9, the data points in general distribute in a narrow range around the average, the standard deviation is about 15 sec for each event.

It would be interesting to examine the relation between the source time τ and the seismic moment M_o. the seismic moments of the four events are listed in Table 6 (Kanamori,1970b,1971; Ben-Menahem and Rosenman, 1972; Wu and Kanamori,1973). The Rat Is. earthquake of 1965 possesses the largest seismic moment of $M_o = 14 \times 10^{28}$ dyne·cm, and the longest source time of τ = 174 sec. The main Kurile event of 1963 has a seismic moment of $M_o = 7.5 \times 10^{28}$ dyne·cm, about a half of that of the Rat Is. earthquake and a source time of τ = 97 sec, about a half of that of the Rat Is. earthquake. Such an approximate propotionality between M_o and τ may be characteristic of ordinary great earthquakes. It is noted that the source times of the Kurile earthquake and the Rat Is. earthquake

are fully explained by the first two terms of equation (7), the rupture time τ_L and the rise time τ_R. In other words, there was no delay for the initiation of the main rupture propagation.

The largest aftershock of the Kurile event and the Tokachi-oki earthquake possess relatively long source times as compared to their seismic moments. If a long source time simply corresponds to a slow source process, it should affect the amplitude behaviour of the seismic waves. For the aftershock of 1963, the low-frequency nature of the seismic waves is apparent and suggests a slow source process (Fukao,1979). Moreover, the zero delay time is suggested from the large initial amplitudes of the long-period P waves (see figures 10, 15, and 16 of Fukao,1979). We therefore try to explain the source time τ = 62 sec by the rupture time τ_L and the rise time τ_R, assuming that $\tau_L = L/v_r$ and $\tau_R = W/2v_r$, where L = 100Km and W = 60 Km (Fukao, 1979). The calculated rupture velocity v_r is 2.1 Km/sec and much smaller than those of the other three great earthquakes (v_r= 3.5 Km/sec). Such a low rupture velocity may be able to suppress the high-frequency component of the seismic waves (Fukao,1979).

For the Tokachi-oki earthquake there is no obvious deficiency of high-frequency seismic waves and a normal rupture velocity (v_r= 3.5 Km/sec) has been estimated

from the long-period surface waves (Kanamori,1971; Fukao and Furumoto,1975). Its long source time should be therefore explained by a delay of the main rupture propagation. The difference between the source time and the sum of the first two terms of equation (7) is about 70 sec; then $\tau - /\tau_L - \tau_R = 65$. This difference corresponds to a delay of about 30 sec. This result is consistent with Fukao and Furumoto (1975) who found a significant time delay of about 40 sec between the onset of the Tokachi-oki earthquake and its main rupturing.

CONCLUSION

We have shown in the present paper that the phase analysis of long-period surface waves is a powerful method for studying source processes of great earthquakes. We have introduced a source time τ which corresponds to the rise time of the source time function of an equivalent point source. We have shown that the source times of great earthquakes can be determined easily and precisely using the complete great-circle phase velocity. This quantity is a unique and useful source parameter to describe the temporal characteristics of great earthquakes.

The initial phase radiation patterns have been

constructed by the phase equalization method using complete great-circle phase velocity data for the great Kurile earthquake of 1963 and its largest aftershock. The phase radiation pattern offers an important information on the source dimension and the focal mechanism. The fault length has been frequently assumed to be nearly equal to the length of the aftershock area within a few days after the main shock. We have shown that this assumption is adequate at least for the great Kurile earthquake.

ACKNOWLEDGEMENT

I would like to thank Ichiro Nakanishi for providing me with the card outputs of the digitized traces of the seismograms, without his support this work would not have been possible. I would also like to thank Dr. Yoshio Fukao for his generous advice and critical comment on the manuscript.

REFERENCES

Abe, K., Tsunami and mechanism of great earthquakes, Phys. Earth Planet. Interiors, 7, 143-153, 1973.

Abe, K., Y. Sato, and J. Frez, Free oscillations of the earth excited by the Kurile Islands earthquake, 1963, Bull. Earthq. Res. Inst. Tokyo Univ., 48, 87-114, 1970.

Aki, K., Accuracy of the Rayleigh wave method for studying the earthquake mechanism, Bull. Earthq. Res. Inst. Tokyo Univ., 40, 91-105, 1962.

Ben-Menahem, A., Radiation of seismic surface waves from finite moving source, Bull. Seism. Soc. Am., 51, 401-435, 1961.

Ben-Menahem, A., and D.G. Harkrider, Radiation pattern of seismic surface waves from burried dipolar point source in a flat stratified earth, J. Geophys. Res., 69, 2605-2620, 1964.

Ben-Menahem, A., H. Jarosch, and M. Rosenman, Large scale processing of seismic data in search of regional and global stress patterns, J. Geophys. Res., 58, 1899-1932, 1968.

Ben-Menahem, A. and M. Rosenman, Amplitude patterns of tsunami waves from submarine earthquakes, J. Geophys. Res., 77, 3097-3128, 1972.

Ben-Menahem, A., M. Rosenman, and D.G. Harkrider, Fast evaluation of source parameters from isolated surface-wave signals part I. Universal tables, Bull. Seism. Soc. Am., 60, 1337-1387, 1970.

Brune, J.N., Radiation pattern of Rayleigh waves from the southeast Alasken earthquake of July 10, 1958, A Symposium on Earthquake Mechanism, Pub. Dominion Obs. Ottawa, 24, 373-383, 1960.

Chandra, U., Analysis of body-wave spectra for earthquake energy determination, Bull. Seism. Soc. Am., 60, 539-563, 1970.

Fukao, Y., Tsunami earthquakes and subduction processes near deep-sea trenches, J. Geophys. Res., in press, 1979.

Fukao, Y. and M. Furumoto, Foreshocks and multiple shocks of large earthquakes, Phys. Earth Planet. Interiors, 10, 355-368, 1975.

Fukao, Y. and M. Furumoto, Stress drops, wave spectra and recurrence intervals of great earthquakes - Implications of the Etorofu earthquake of 1958 November 6, Geophys. J. Roy. Astron. Soc., 57, 23-40, 1979.

Hagiwara, T., A note on the theory of the electro-magnetic seismograph, Bull. Earthq. Res. Inst. Tokyo Univ., 36, 139-164, 1958.

Haskell, N.A., Total energy and energy spectral density of elastic wave radiation from propagating faults, Bull. Seism. Soc. Am., 54, 1811-1841, 1964.

Hatori, T., An investigation of the tsunami generated by the east Hokkaido earthquake of August, 1969, Bull. Earthq. Res. Inst. Tokyo Univ., 48, 399-412, 1970.

Kanamori, H., Velocity and Q of mantle waves, Phys. Earth Planet. Interiors, 2, 259-275, 1970a.

Kanamori, H., Synthesis of long-period surface waves and its application to earthquake source studies - Kurile Islands earthquake of October 13, 1963, J. Geophys. Res., 75, 5011-5027, 1970b.

Kanamori, H., Focal mechanism of Tokachi-oki earthquake of May 16, 1968, Tectonophysics, 12, 1-13, 1971.

Nakanishi, I., Measurements of phase velocity and Q of mantle Rayleigh waves, Master Thesis Nagoya Univ. Nagoya, Japan, 1978a.

Nakanishi, I., Regional differences in the phase velocity and the quality factor Q of mantle Rayleigh waves, Science, 200, 1379-1381,1978b.

Nakanishi, I., Phase velocity and Q of mantle Rayleigh waves, Geophys. J. Roy. Astron. Soc., in press,1979.

Plafker, G., Alaskan earthquake of 1964 and Chilean earthquake of 1960: Implications for arc tectonics, J. Geophys. Res., 77, 901-925, 1972.

Savage, J.C., Relation of corner frequency to fault dimensions, J. Geophys. Res., 77, 3788-3795, 1972.

Shimazaki, K., Nemuro-oki earthquake of June 17, 1973; A lithospheric rebound at the upper half of the interface, Phys. Earth Planet. Interiors, 9, 314-327, 1974.

Stauder, W. and L. Mualchin, Fault motion in the large earthquakes of the Kurile-Kamchatka arc and the Kurile-Hokkaido corner, J. Geophys. Res., 81, 297-308, 1976.

Wu, F.T. and H. Kanamori, Source mechanism of February 4, 1965, Rat Island earthquake, J. Geophys. Res., 78, 6082-6092, 1973.

Table 1. List of earthquakes

Earthquake	Date	Time	Latitude (°N)	Longitude (°E)	Depth (Km)	Magnitude M_S
Kurile [a]	Oct.13,1963	05h17m57s	44.8	149.5	60	$7\frac{3}{4} - 8\frac{1}{2}$
The largest aftershock [b]	Oct.20,1963	00h53m11s	44.87	150.32	26	7.1 [c]
Rat Is. [a]	Feb.04,1965	05h01m22s	51.3	178.6	40	7.8
Tokachi-oki [a]	May 16,1968	00h48m55s	40.8	143.2	7	7.9

a) U.S. Coast Geodetic Survey; b) International Seismological Summary (ISS);
c) Pasadena and Palisades.

Table 2. Derivation of R wave initial phase and source time τ of the Kurile earthquake of October 13, 1963.

Station	Azimuth (°)	Distance (Km)	Great-circle (Km)	Signal 1	Initial phase (radian)	Signal 2	Initial phase (radian)	Source time τ (sec)	Magnification
AAE	291.3	10898	40039	R3	4.94	R4	6.13	119	750
ADE	189.0	8901	40010	R3	5.59	R4	6.48	68	750
AFI	139.0	7587	40024	R3	5.91	R2	5.73	102	750
ATU	320.0	9357	40024	R5	6.05	R4	5.87	85	1500
BUL	277.1	13985	40043	R3	5.20	R4	6.60	88	1500
COP	336.3	8164	40014	R5	5.79	R4	5.62	103	750
GDP	8.8	7215	40010	R3	6.15	R2	5.63	89	750
GOL	51.3	8036	40030	R3	5.85*	R2	4.93*	117	1500
IST	318.6	8807	40024	R3	5.67	R4	6.04	89	1500
KON	339.8	7862	40013	R5	5.94	R4	5.83	98	1500
KTG	356.8	7208	40009	R3	6.09	R2	5.55	100	1500
LPS	57.2	11200	40033	R3	5.56*	R2	5.05*	130	750
NAI	285.7	11885	40041	R3	5.15	R4	6.20	104	1500
NDI	280.4	6479	40042	R3	5.55	R4	6.35	93	1500
PRE	272.0	14410	40043	R3	5.58	R4	6.68	74	1500

Table 2 (continued)

Station	Azimuth	Distance	Great-circle	Signal 1	Initial phase	Signal 2	Initial phase	Source time τ	Magnification
SHI	296.2	8223	40036	R3	5.26	R4	6.53	84	1500
TOL	340.0	10261	40013	R5	6.11	R4	5.89	94	1500
TUC	60.0	8249	40035	R3	6.01*	R4	5.38*	110	1500
AAM	36.8	9011	40021	R3	5.96				1500
ANP	238.5	3326	40034			R2	6.06*		750
ARE	63.5	15071	40037	R3	5.64*				1500
BEC	28.5	10787	40017	R3	6.46				1500
DAL	51.0	9118	40030	R3	5.66*				1500
DUG	55.0	7528	40032			R4	5.09*		3000
GEO	34.5	9631	40020	R3	6.33				1500
HNR	167.3	6097	40011			R4	5.77		1500
LAH	284.9	6512	40041			R4	6.12		750
MDS	39.8	8616	40023	R3	6.60				1500
PDA	356.0	10850	40009	R3	6.07				750
QUE	288.0	7164	40040			R4	6.05		3000
QUI	57.6	13187	40034	R3	5.39*				1500
RAB	176.5	5433	40009			R2	5.80		750
SHA	46.6	9818	40027	R3	6.08				1500
TAU	181.6	9718	40009			R2	6.01		750

The values with * are excluded from the radiation pattern analysis.

The period T_p of the free oscillation of pendulum is T_p=30 sec.

Table 3. Derivation of R wave initial phase and source time τ of the largest aftershock of the Kurile earthquake of 1963.

Station	Azimuth (°)	Distance (Km)	Great-circle (Km)	Signal 1	Initial phase (radian)	Signal 2	Initial phase (radian)	Source time τ (sec)	Magnification
ALQ	56.0	8278	40032	R3	5.69	R2	5.88	80	3000
ARE	64.3	15009	40037	R3	6.14	R2	6.25	75	1500
BAG	231.0	4206	40030	R3	6.23	R2	5.61	81	1500
FLO	43.6	8931	40025	R3	6.07	R2	6.55	57	1500
GDH	9.1	7197	40010	R3	5.69	R2	6.84	68	750
HNR	168.3	6091	40011	R3	6.86	R2	5.69	68	3000
IST	319.0	8844	40024	R3	5.88	R2	6.45	81	1500
KEV	340.1	6489	40013	R3	6.14	R2	6.94	45	1500
MDS	40.3	8568	40023	R3	6.14	R2	6.50	47	1500
PTO	344.4	10250	40012	R3	6.10	R2	6.69	47	750
SHA	47.1	9766	40027	R3	6.78	R2	6.85	32	1500
STU	335.2	8964	40015	R3	5.61	R2	6.51	64	750

The period T_p of of the free oscillation of pendulum is T_p=30 sec.

Table 4. Derivation of source time $\bar{\tau}$ of the Rat Island earthquake of February 4, 1965.

Station	Azimuth (°)	Distance (Km)	Great-circle (Km)	Signals	Source time τ (sec)	Magnification
AAE	317.3	12295	40021	R5,R6	152	1500
ADE	211.9	10322	40016	R5,R6	190	750
AKU	7.7	6953	40010	R2,R3	163	375
ATU	340.5	9817	40012	R4,R5	174	1500
COP	351.9	8077	40010	R4,R5	170	375
GEO	54.2	7616	40026	R3,R4	155	750
GDH	20.4	5977	40012	R3,R4	168	750
HNR	200.9	6964	40012	R2,R3	182	750
JER	329.6	10132	40016	R4,R5	168	1500
KEV	348.7	6381	40010	R5,R6	144	750
KTG	8.0	6402	40010	R4,R5	194	750
MAL	2.4	10248	40009	R4,R5	150	1500
PTO	5.4	9739	40009	R4,R5	200	750
TAU	202.7	10868	40013	R3,R4	170	750
TOL	2.0	9899	40009	R5,R6	199	1500
VAL	5.6	8538	40009	R4,R5	201	750

The period T_p of the free oscillation of pendulum is T_p=30 sec.

Table 5. Derivation of source time τ of the Tokachi-oki earthquake of May 16, 1968.

Station	Azimuth (°)	Distance (Km)	Great-circle (Km)	Signals	Source time τ (sec)	Magnification
AFI	132.4	7630	40030	R2,R3	107	750
ANP	235.9	2656	40036	R3,R4	111	750
AQU	325.3	9505	40022	R3,R4	96	3000
HKC	241.8	3412	40039	R2,R3	130	750
LPB	56.9	15981	40037	R3,R4	132	1500
NDI	279.3	6048	40046	R3,R4	92	1500
NNA	61.9	14974	40040	R3,R4	120	3000
POO	271.5	6967	40048	R3,R4	113	1500
PRE	264.8	13883	40048	R3,R4	127	1500
SNG	240.5	5627	40038	R3,R4	125	3000

The period T_p of the free oscillation of pendulum is T_p=15 sec.

Table 6. List of source parameters.

Earthquake	Seismic moment M_o 10^{28} dyn·cm	Fault length L, Km	Fault width W, Km	Rupture velocity v_r, Km/sec	Source time τ, sec	Rupture time $\sqrt{\tau_L}$, sec	Rise time $\sqrt{\tau_R}$, sec	Delay time $\sqrt{\tau_D}$, sec
Kurile[(a)]	7.5	250	150	3.5	97	70	20	+
Aftershock[(b)]	0.7	100	60	2.1	62	40	20	0
Rat Is.[(c)]	14	500	150	3.5	174	140	20	+
Tokachi-oki[(d)]	2.8	150	100	3.5	115	40	10	30

(a) Kanamori (1970 b) and Ben-Menahem and Rosenman (1972),

(b) Fukao (1979),

(c) Ben-Menahem and Rosenman (1972) and Wu and Kanamori (1973),

(d) Kanamori (1971).

FIGURE CAPTION

Fig.1. Azimuthal plot of the initial phases of the R waves from the Kurile earthquake of 1963. The initial phases are indicated on the unit of radian. The solid and open circles show the average values at the period around T=250 sec. For explanation of the open circles, see the text. The solid curve is the best fitted cosine function curve whose amplitude is 0.65 (radian). The constant term of -0.39 (radian) has been determined by summing the initial phases of the R_n and R_{n+1} waves by the technique described in the text.

Fig.2. Aftershock areas for the Kurile earthquake of Oct.13, 1963, its largest foreshock (Oct.12), and its largest aftershock (Oct.20) (from Fukao, 1979). Open circles denote the earthquakes which occurred during the interval of the largest foreshock and the main shock. Crosses represent the earthquakes which occurred within three days after the largest aftershock. For the largest aftershock, the epicentre locations by International Seismological Summary (ISS) and U.S. Coast and Geodetic Survey (USCGS) are indicated.

Fig.3. Azimuthal plot of the initial phases of the R waves from the largest aftershock of the Kurile earthquake of 1963. The phases are indicated on the unit of radian. The solid curve shows the finiteness factor for a fault which propagates southwards over a fault length of 100 Km. The dotted curve shows the focal mechanism factor for a thrust fault with a dip-angle of $\delta = 3°$ and a dip-direction of $\phi = 315°$. The source depth is assumed to be 10 Km. The thin line represents the constant term of the focal mechanism factor ($\pi/4$).

Fig.4. Schematic explanation of the relation among the source time τ, the rupture time τ_L, the rise time τ_R, the delay time τ_D, and the seismic moment M_o. The time t=0 corresponds to the origin time of the earthquake.

Fig.5. Diagram of source time τ versus period for the Kurile earthquake of 1963. Three stations (AAE, ADE, KON) are selected. AAE (solid circles) gives the second longest estimation of the source time of τ=119 sec, and ADE (open circles) the shortest estimation of τ =68 sec for the event.

Fig.6. Azimuthal plot of the observed source times τ for the Kurile earthquake of 1963. The solid line represents the average value. The standard deviation of the data is 15 sec.

Fig.7. Azimuthal plot of the observed source time τ for the largest aftershock of the Kurile event of 1963. The solid line represents the average value. The standard deviation of the data is 16 sec.

Fig.8. Azimuthal plot of the observed source time τ for the Rat Is. earthquake of 1965. The solid line represents the average value. The standard deviation of the data is 19 sec.

Fig.9. Azimuthal plot of the observed source time τ for the Tokachi-oki earthquake of 1968. The solid line represents the average value. The standard deviation of the data is 14 sec.

Figure 1

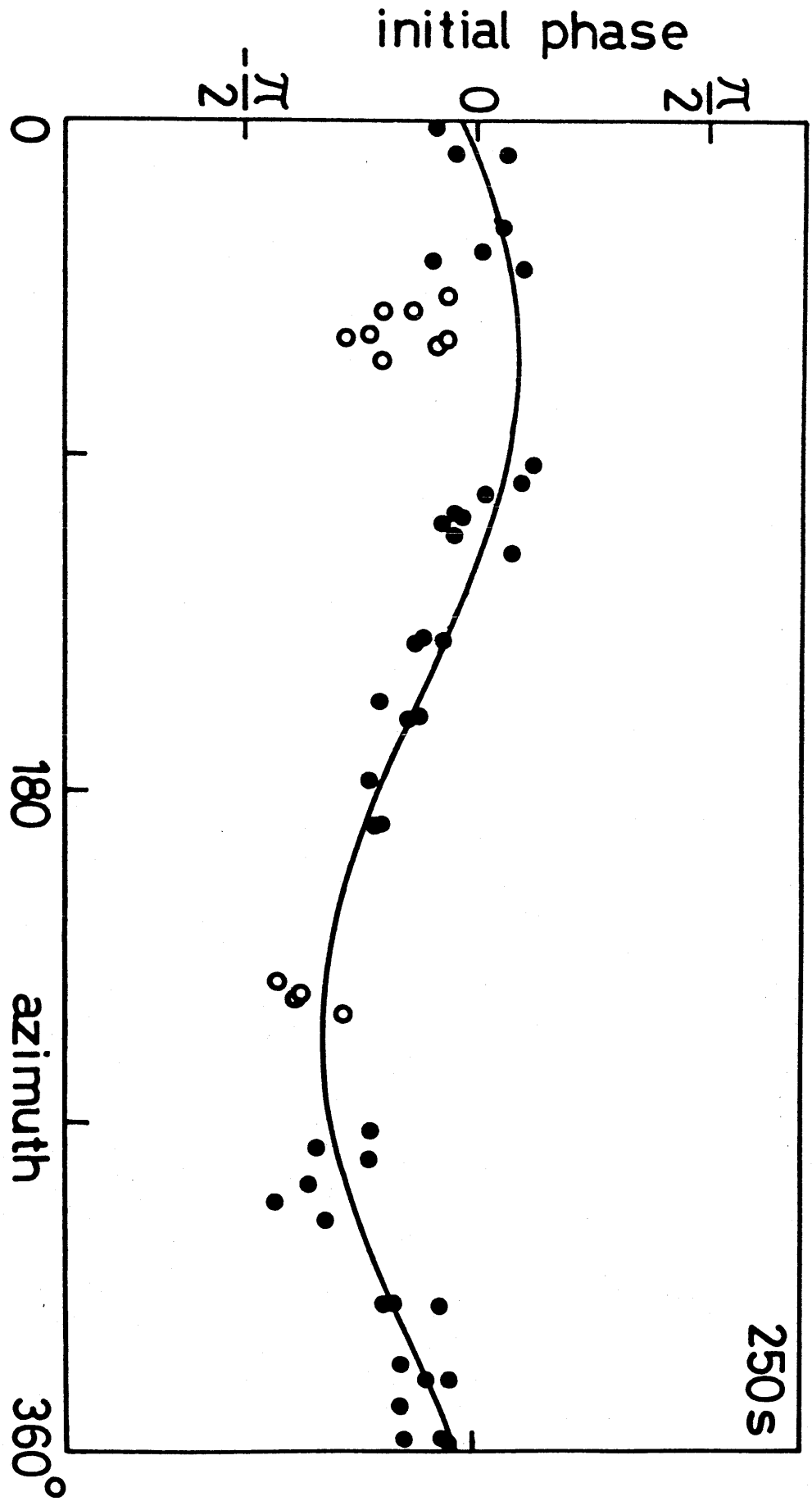

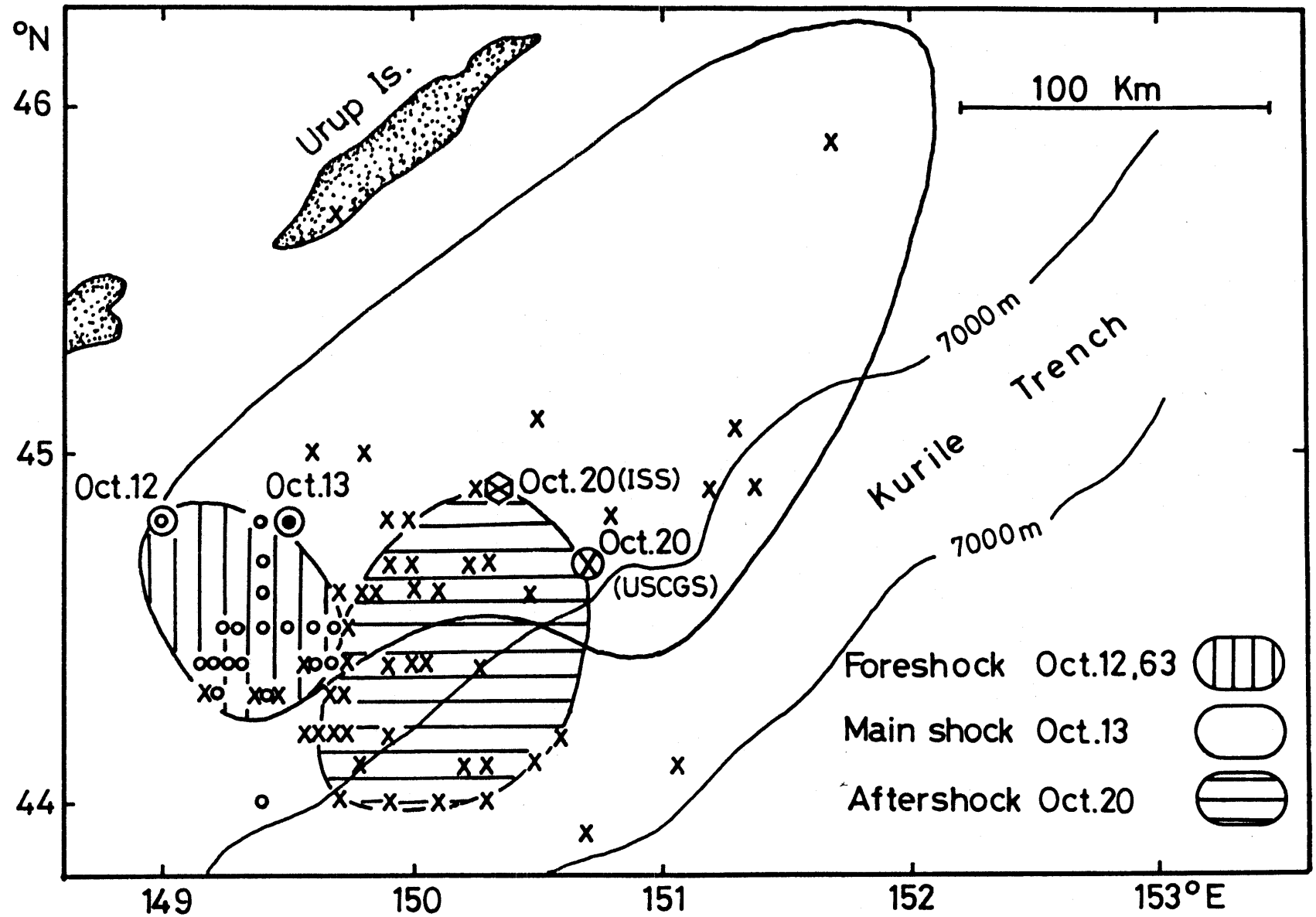
°N
46
45
44
149
150
151
152
153°E
Urup Is.
100 Km
7000m
Kurile Trench
7000m
Oct.12
Oct.13
Oct.20(ISS)
Oct.20
(USCGS)
Foreshock Oct.12,63
Main shock Oct.13
Aftershock Oct.20

Figure 2

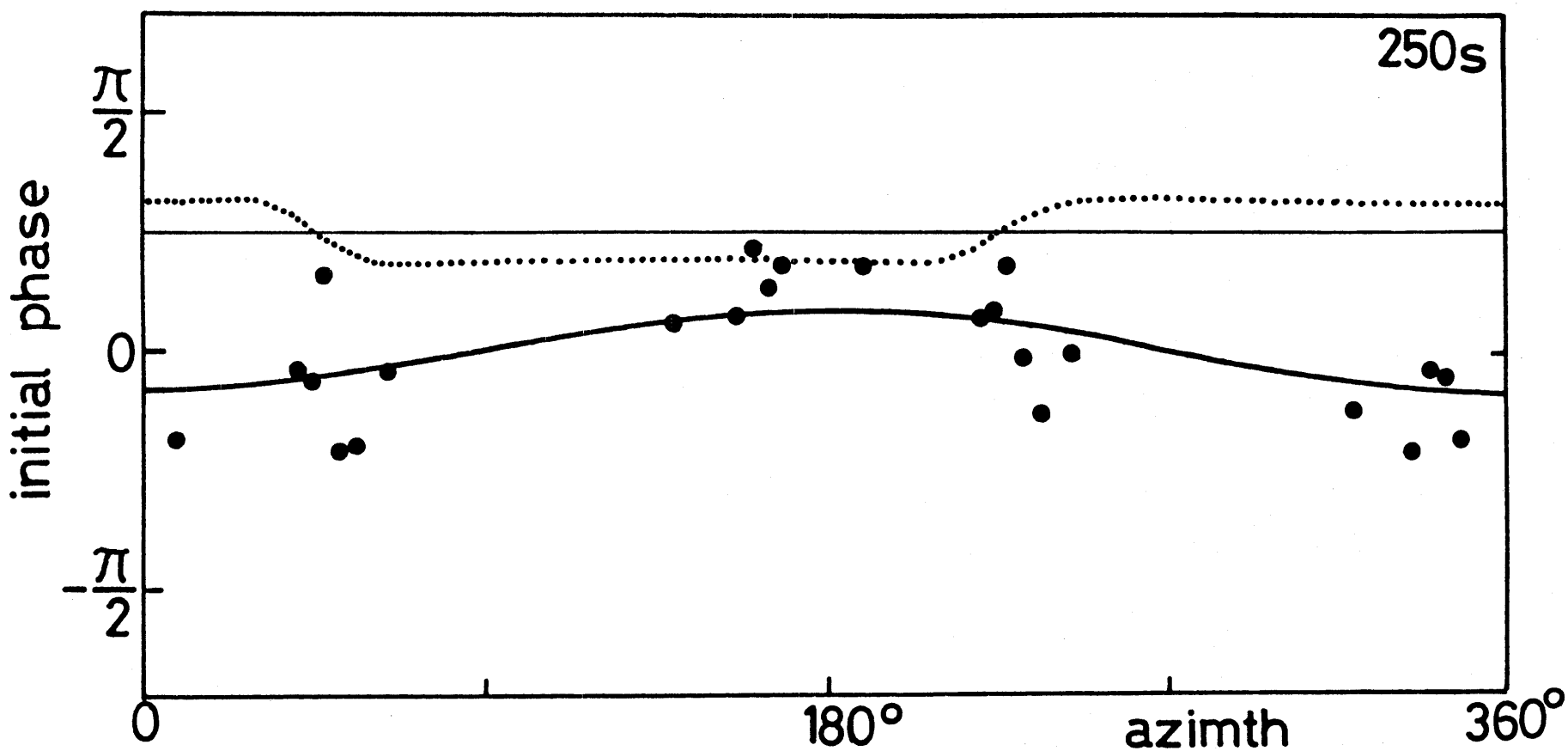

Figure 3

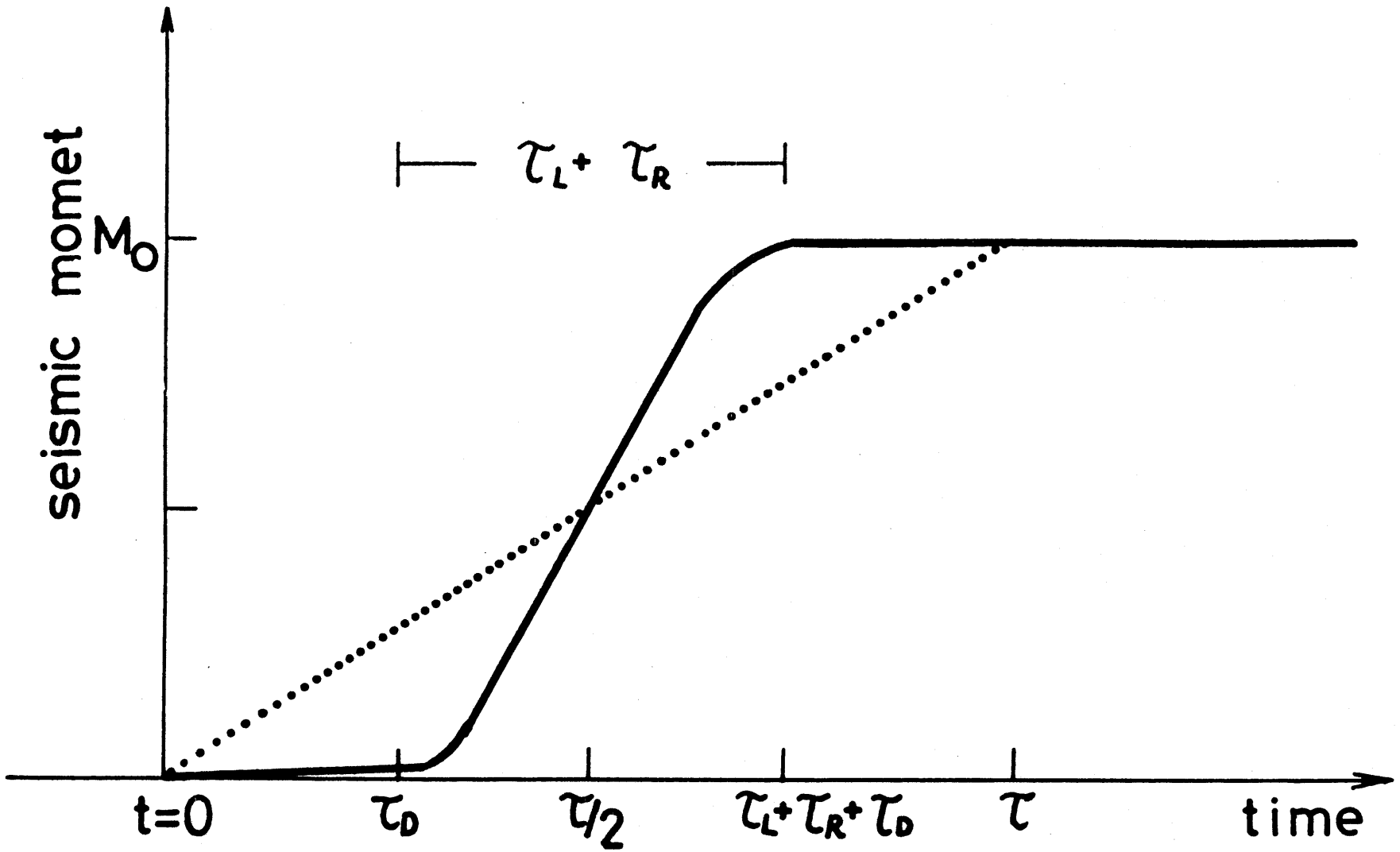
seismic momet
M_0
$\tau_L + \tau_R$
t=0
τ_D
$\tau/2$
$\tau_L+\tau_R+\tau_D$
τ
time

Figure 4

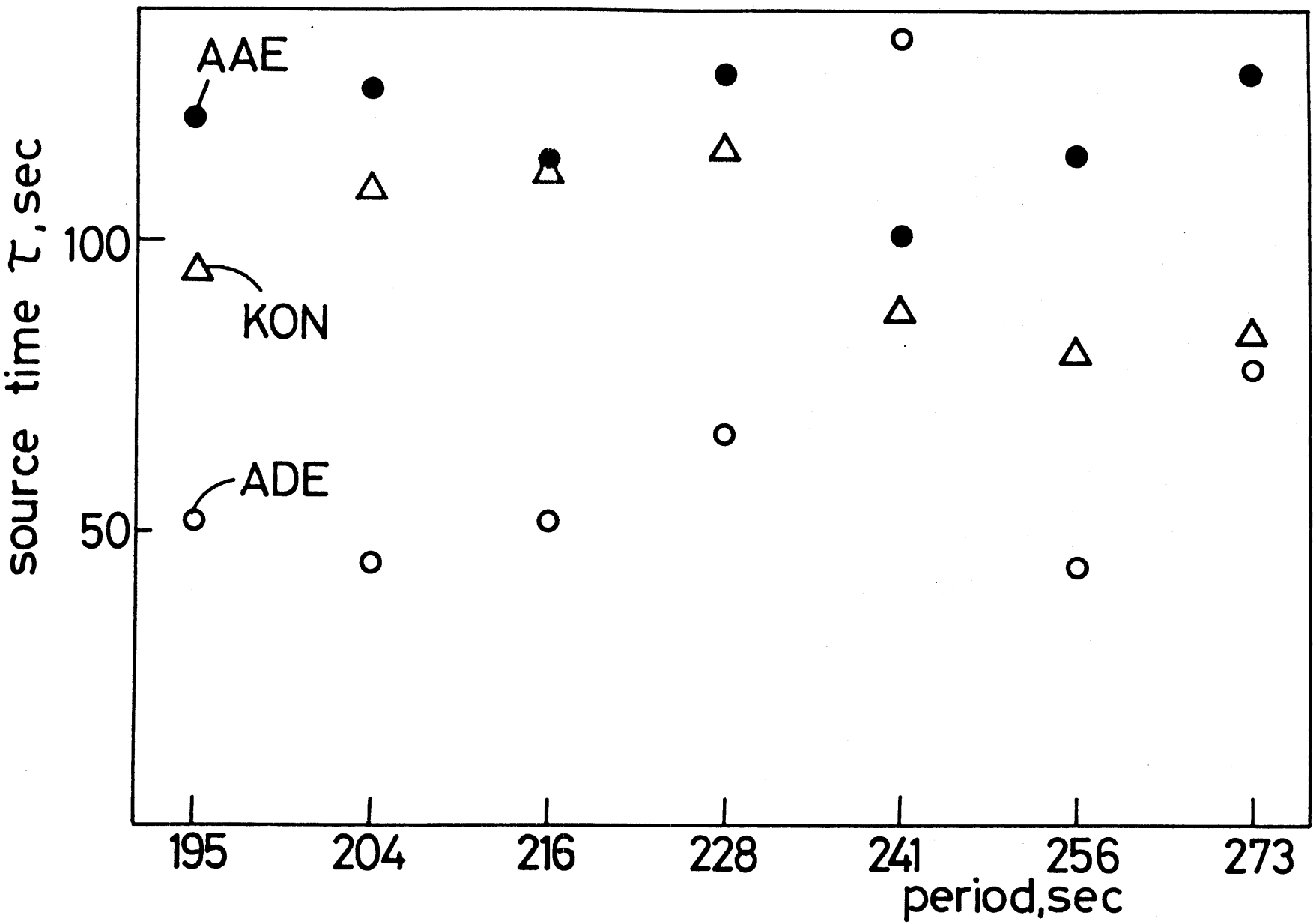
AAE
KON
ADE
source time τ, sec
100
50
195
204
216
228
241
256
273
period, sec

Figure 5

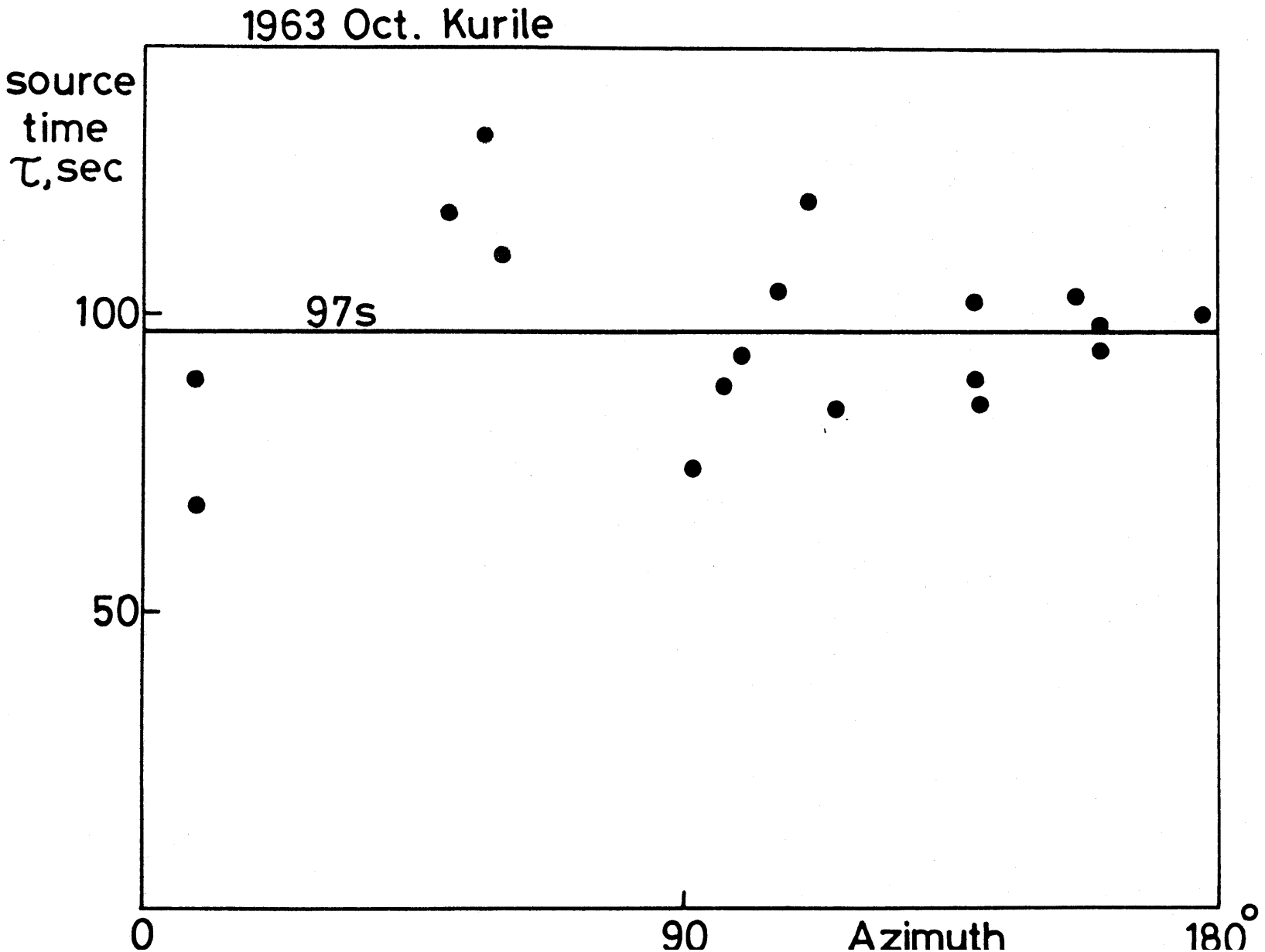

Figure 6

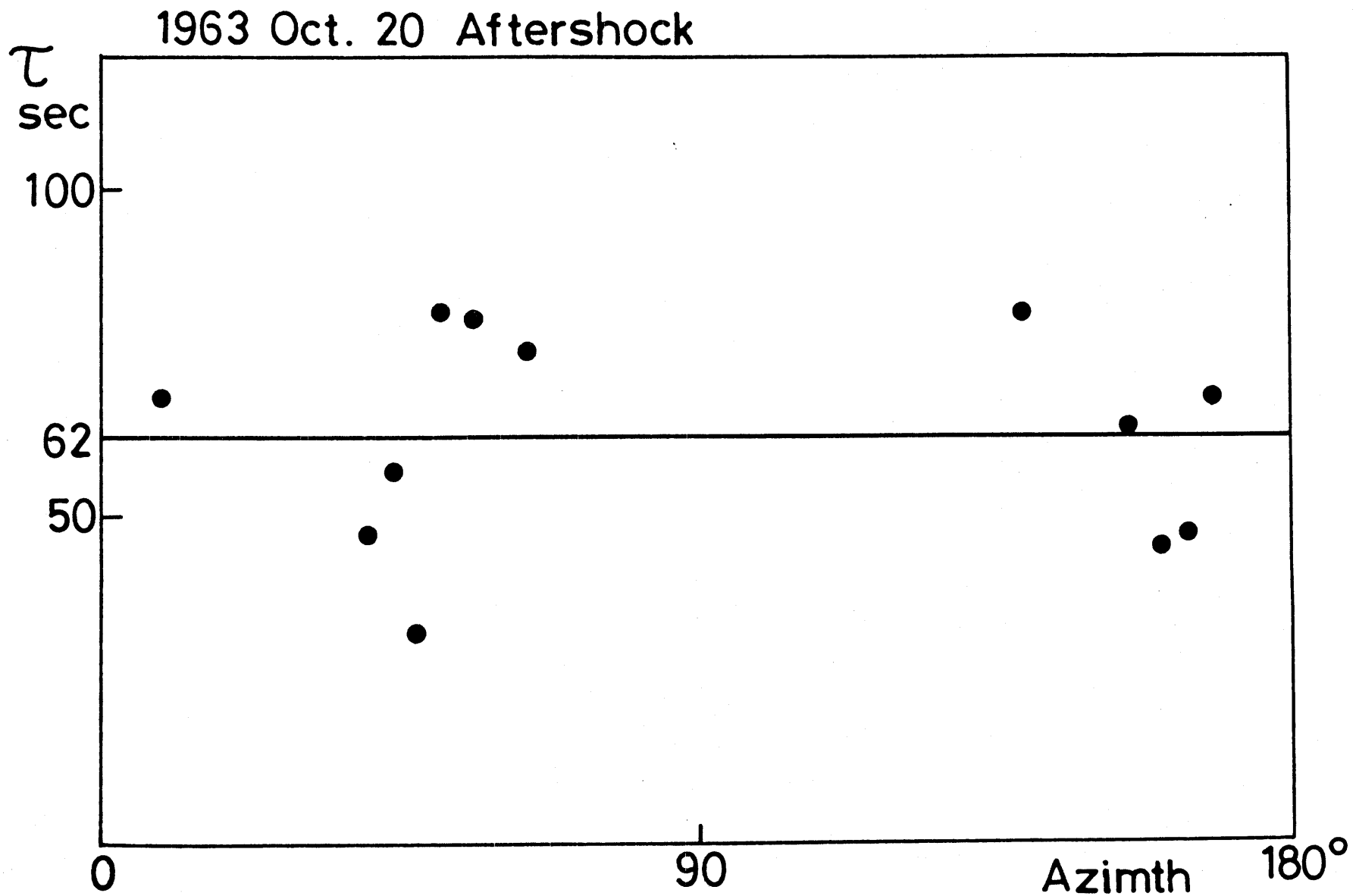

Figure 7

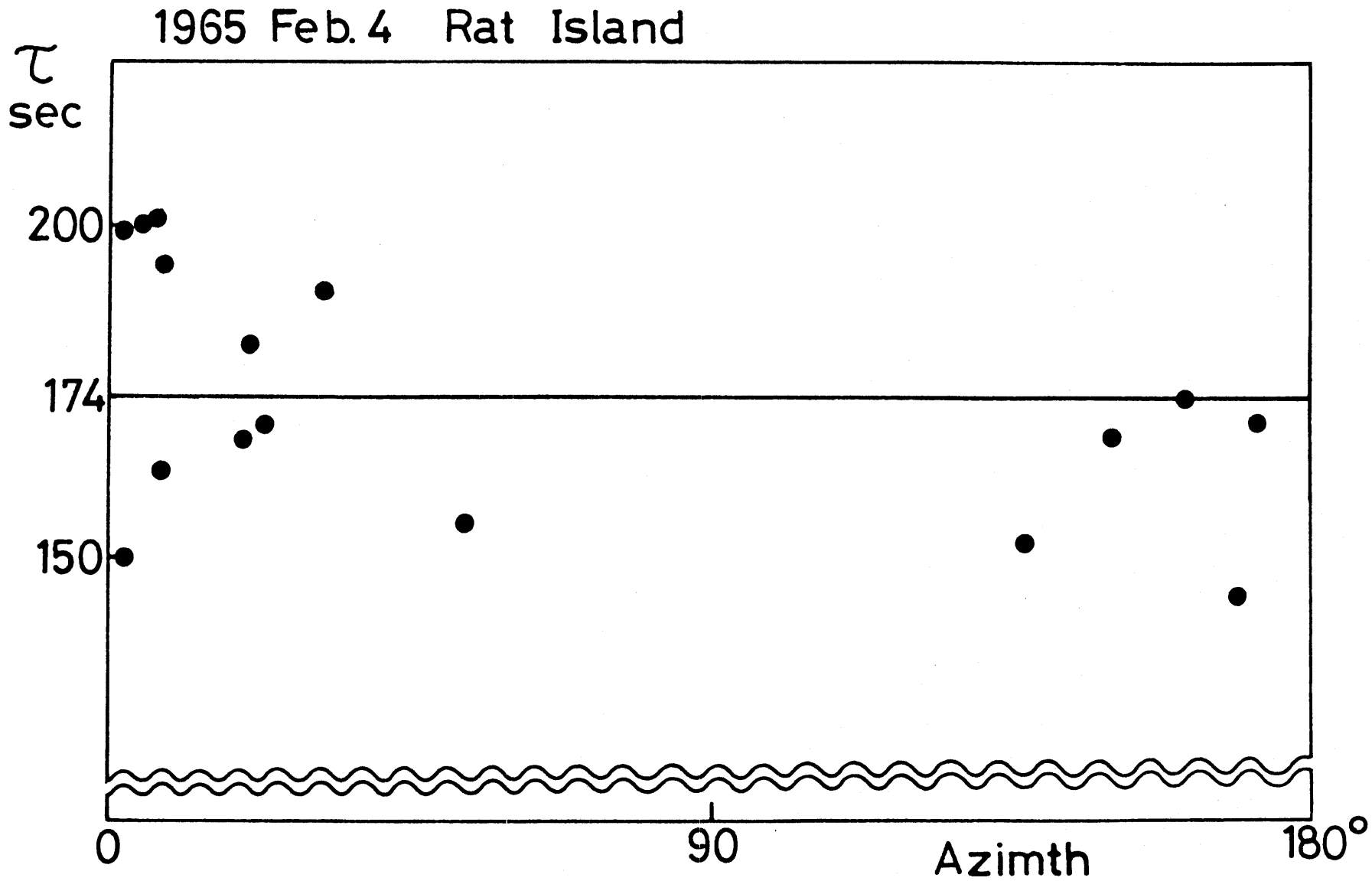

Figure 8

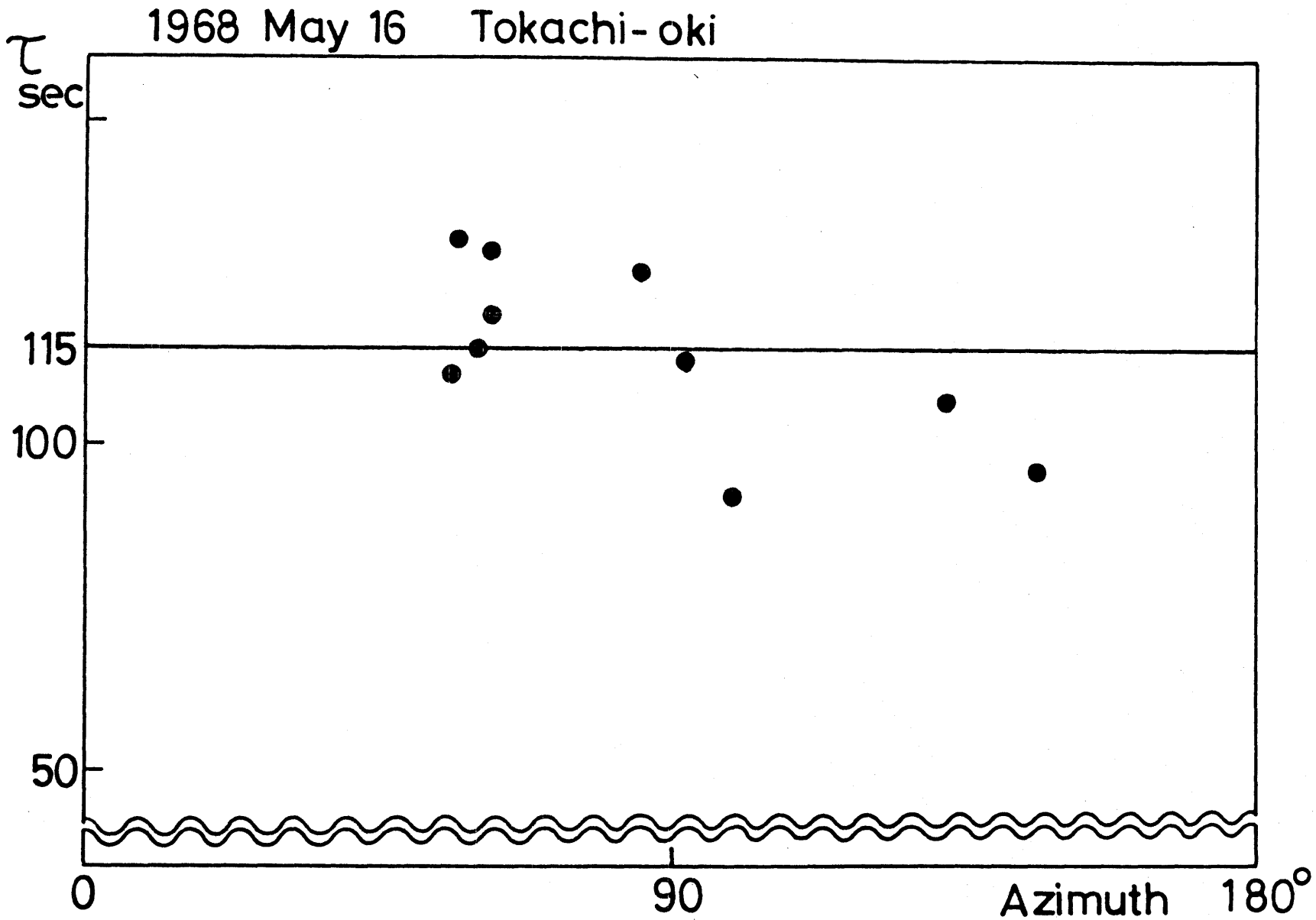

Figure 9